

AFF-1 infection mechanism is fundamentally different from that of native VSV. Whereas the infection of VSV is mediated by VSVG only on the viral membrane, infection mediated by VSVΔG–AFF-1 requires an FF protein on both the viral membrane and the cell membrane.

To study the relation between structure and function of AFF-1, we used transmission electron microscopy (TEM). We compared negatively stained samples of VSVΔG to VSVG- and AFF-1-complemented VSVΔG preparations (11). VSVΔG virions have the typical VSV shape with a smooth membrane (hence, they are termed “bald”), whereas both VSVΔG-G (19) and VSVΔG–AFF-1 virions displayed distinct spikes on their envelopes (Fig. 4, A to C). In negative stain (pH 5), VSVG forms elongated spikes on VSVΔG-G (Fig. 4B) (19), whereas VSVΔG–AFF-1 showed shorter spikes (Fig. 4C). The estimated average spike lengths of VSVG and AFF-1 were 145 and 109 Å, respectively (table S2). To confirm that the observed spikes were indeed AFF-1, we used anti-AFF-1 polyclonal antibodies to perform immunogold labeling. We observed specific immunoreactivity on the surface of VSVΔG–AFF-1 (Fig. 4, D and E, and figs. S7 and S8). To further characterize the pseudoviruses at higher resolution and in a more native state, we used cryogenic TEM (cryo-TEM) (Fig. 4, F to H) and cryogenic electron tomography (cryo-ET) (Fig. 4, I to K, and movie S3) to image them embedded in vitreous ice. Cryo-TEM projection images showed that AFF-1 proteins coat the pseudoviruses. Side views of individual spikes could be observed at central sections of the tomograms

(Fig. 4J). Higher-order assemblies of AFF-1 in the form of penta- or hexameric “flower-shaped” supercomplexes could be observed in slices through the tomogram oriented peripheral to the pseudotyped virus particles (Fig. 4I). These assemblies were more visible in slices through the tomograms of copurified vesicles (Fig. 4, L and M, fig. S9, and movies S4 and S5). The order of these arrays may have a critical function in bending and deforming plasma membranes to mediate fusion.

Here, we have presented evidence that FF proteins are functionally conserved in evolution and can restore the infectivity of VSVΔG through interactions with FF proteins on the target cell. Thus, FF, viral, and intracellular fusogens converge functionally as minimal fusion machines that function on their own to promote fusion.

#### References and Notes

1. W. Wickner, R. Schekman, *Nat. Struct. Mol. Biol.* **15**, 658 (2008).
2. S. Martens, H. T. McMahon, *Nat. Rev. Mol. Cell Biol.* **9**, 543 (2008).
3. J. M. White, S. E. Delos, M. Brecher, K. Schornberg, *Crit. Rev. Biochem. Mol. Biol.* **43**, 189 (2008).
4. A. Sapir, O. Avinoam, B. Podbilewicz, L. V. Chernomordik, *Dev. Cell* **14**, 11 (2008).
5. M. Oren-Suissa, B. Podbilewicz, *Trends Cell Biol.* **17**, 537 (2007).
6. E. H. Chen, E. Grote, W. Mohler, A. Vignery, *FEBS Lett.* **581**, 2181 (2007).
7. W. A. Mohler *et al.*, *Dev. Cell* **2**, 355 (2002).
8. A. Sapir *et al.*, *Dev. Cell* **12**, 683 (2007).
9. B. Podbilewicz *et al.*, *Dev. Cell* **11**, 471 (2006).
10. G. Shemer *et al.*, *Curr. Biol.* **14**, 1587 (2004).
11. Materials and methods are available as supporting material on Science Online.

12. J. Závada, *J. Gen. Virol.* **15**, 183 (1972).
13. M. J. Schnell, L. Buonocore, E. Kretzschmar, E. Johnson, J. K. Rose, *Proc. Natl. Acad. Sci. U.S.A.* **93**, 11359 (1996).
14. A. Takada *et al.*, *Proc. Natl. Acad. Sci. U.S.A.* **94**, 14764 (1997).
15. Y. Matsuura *et al.*, *Virology* **286**, 263 (2001).
16. S. Fukushi *et al.*, *J. Gen. Virol.* **86**, 2269 (2005).
17. L. Lefrançois, D. S. Lyles, *Virology* **121**, 157 (1982).
18. C. Hu *et al.*, *Science* **300**, 1745 (2003).
19. S. Libersou *et al.*, *J. Cell Biol.* **191**, 199 (2010).

**Acknowledgments:** We thank I. Nagano, M. Whitt, A. Fire, C. Giraud, and J. Rothman for reagents; F. Glaser, M. Glickman, A. Harel, O. Kleinfeld, T. Schwartz, I. Sharon, E. Spooner, R. Sommer, and members of the White and Podbilewicz labs for discussions; the Smoler Proteomics Center at the Technion and the Whitehead Institute for Biomedical Research for mass spectrometry; T. Ziv for proteomics analysis; the Caenorhabditis Genetics Center for nematode strains; and I. Yanai and A. de Silva for critically reading the manuscript. This work was supported by grants from the FIRST Program of the Israel Science Foundation (ISF 1542/07 to B.P.), the Human Frontier Science Program (RG0079/2009-C to K.G.), and the NIH (AI22470 to J.M.W.), as well as a Wellcome Trust Senior Research Fellowship to K.G. The Technion Research and Development Foundation has filed a patent relating to methods and compositions useful in cell-cell fusion using FF proteins of nematode origin and to antinematodal methods and compositions, using proteins of the nematode fusion family.

#### Supporting Online Material

www.sciencemag.org/cgi/content/full/science.1202333/DC1  
Materials and Methods  
Figs. S1 to S9  
Tables S1 to S5  
References  
Movies S1 to S5

29 December 2010; accepted 14 March 2011  
Published online 24 March 2011;  
10.1126/science.1202333

## The Spatial Periodicity of Grid Cells Is Not Sustained During Reduced Theta Oscillations

Julie Koenig, Ashley N. Linder, Jill K. Leutgeb, Stefan Leutgeb\*

Grid cells in parahippocampal cortices fire at vertices of a periodic triangular grid that spans the entire recording environment. Such precise neural computations in space have been proposed to emerge from equally precise temporal oscillations within cells or within the local neural circuitry. We found that grid-like firing patterns in the entorhinal cortex vanished when theta oscillations were reduced after intraseptal lidocaine infusions in rats. Other spatially modulated cells in the same cortical region and place cells in the hippocampus retained their spatial firing patterns to a larger extent during these periods without well-organized oscillatory neuronal activity. Precisely timed neural activity within single cells or local networks is thus required for periodic spatial firing but not for single place fields.

Brain oscillations are thought to be essential for neural computations and for organizing cognitive processes (1–5). Yet it has been difficult to distinguish computations in neural circuits that require oscillatory neural activity from those that occur irrespective of the precise temporal organization that oscillatory rhythms can

provide. Theta oscillations (4 to 11 Hz) can be recorded in the local field potential of the hippocampus and the parahippocampal cortices, including the entorhinal cortex. These brain regions are important for memory and navigation (6) and contain a number of different cell types with precise spatial firing patterns, such as place cells,

head-direction cells, and grid cells (7–9). Grid cells are found in the medial entorhinal cortex (MEC), parasubiculum, and presubiculum and have multiple firing peaks that form a highly regular hexagonal firing pattern in two-dimensional space (8, 10).

The coexistence of cells with well-defined spatial firing patterns and of theta oscillations that are particularly prominent during voluntary movement (11) suggests that oscillatory brain activity might be essential for spatial computations. In particular, it has been proposed that precisely tuned theta oscillations, as an animal moves through its environment, might be necessary for generating the periodic spatial firing of grid cells. Such spatial regularity might arise from interference between oscillators with small frequency differences, given that those oscillators are controlled by both movement velocity and movement direction (12–14). Although the oscillators could be implemented in various ways in single neurons or

Neurobiology Section and Center for Neural Circuits and Behavior, Division of Biological Sciences, University of California, San Diego, USA.

\*To whom correspondence and requests for materials should be addressed. E-mail: sleutgeb@ucsd.edu

**Fig. 1.** Field theta oscillations in the MEC and hippocampus were reduced after microinfusion of lidocaine into the medial septal area [red arrows in (A) to (C) and (E)]. **(A)** Behavioral design. Each of the four 10-min recording sessions is referred to as 1 to 4. **(B)** Time-frequency plots and raw LFP traces show the simultaneous reduction in theta power in the MEC and hippocampus. The raw traces are from periods with running speeds above 15 cm/s. **(C)** For experiments with recordings of cells in either the MEC (black) or hippocampus (blue), the percent change in the power of LFP oscillations between 7 and 9 Hz is shown compared to baseline. Each 10-min recording was subdivided into two 5-min intervals (a and b). **(D)** The peak frequency of remaining oscillations in the theta range decreased (hippocampus:  $t = 3.37$ ,  $P < 0.01$ ; MEC:  $t = 3.67$ ,  $P < 0.01$ ). **(E)** Average running speed during all sessions with single-unit recordings. Because the running speed before and after the lidocaine infusion was the same ( $t = -1.97$ , n.s.), the reduced theta power was not a consequence of reduced movement velocity.

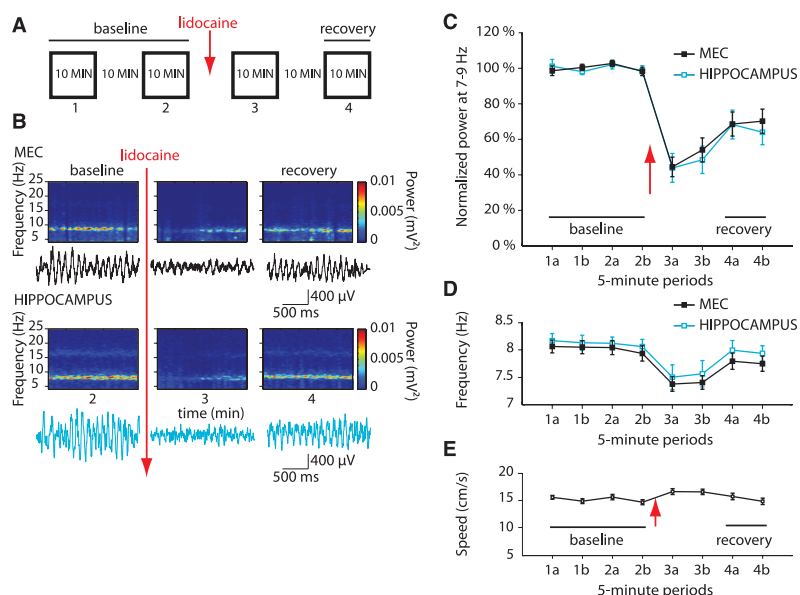
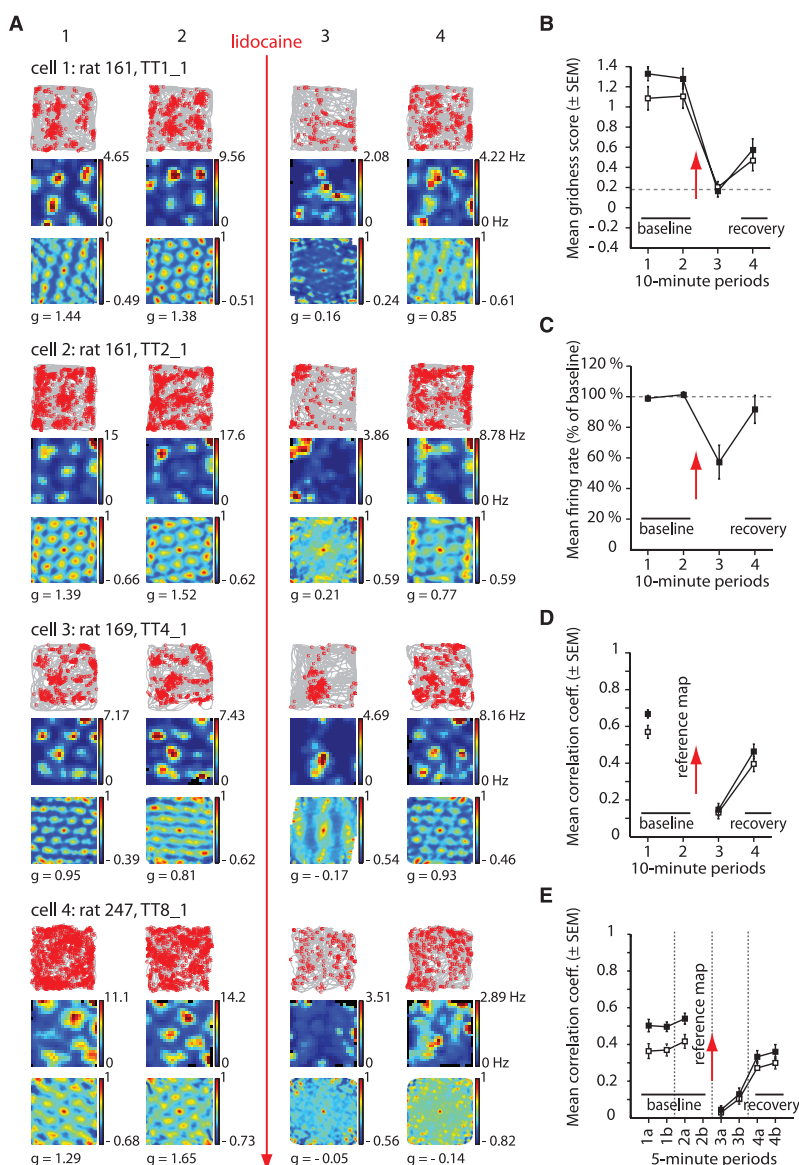


**Fig. 2.** The spatial periodicity of grid cells in the MEC vanished during periods of reduced theta activity. **(A)** Firing correlates for four representative MEC grid cells (see fig. S3 for additional examples). Cells 1 and 2 were recorded simultaneously. Trajectories (gray) with superimposed spike locations (red dots) are shown in the top row of each cell's panel. The corresponding color-coded rate maps and spatial autocorrelation matrices compose the middle and bottom rows, respectively. The color scale for rate maps (shown for each 10-min recording interval) is from 0 Hz to the peak rate, and for the spatial autocorrelation matrices is from the minimum correlation coefficient to 1. **(B)** In the original (solid symbols) and subsampled data (open symbols), the mean gridness score decreased to chance levels (stippled line) after septal inactivation ( $n = 26$ ;  $t = -0.64$  and  $0.18$ , n.s. compared to chance;  $t = 11.89$  and  $7.16$ ,  $P < 0.001$  as compared to the score before inactivation). Although grid cell firing rates completely recovered after the infusion, the recovery of gridness was variable across the recorded population (see also fig. S6). **(C)** The mean firing rates for all recorded grid cells are shown as the percent change compared to baseline rates. Firing rates decreased after septal lidocaine infusions ( $t = 3.19$ ,  $P < 0.001$ ). **(D)** Spatial correlation coefficients between rate maps. The rate map for the session before lidocaine infusion (session 2) served as a reference map to which all others were compared, and therefore is not plotted. Grid cell firing after lidocaine infusion compared to baseline did not remain at corresponding locations after theta reduction ( $t = 12.84$ ,  $P < 0.001$ ). **(E)** During the 5-min period of the maximal drug effect, the spatial maps were completely uncorrelated to the period before the lidocaine infusion (original and subsampled data,  $t = 2.04$  and  $1.28$ , n.s. compared to zero;  $t = 11.8$  and  $t = 9.92$ ,  $P < 0.001$  compared to baseline).



local circuits, at least one of them would likely be phase-locked to theta oscillations. We tested the hypothesis that reducing theta oscillations by inactivating inputs from the subcortical pacemakers in the medial septal area (15–18) would disrupt the spatial computations of grid cells.

To explore the effects of reduced theta oscillations on spatial firing patterns, we trained 14 rats to randomly forage in a 1.2-m-by-1.2-m box and recorded the local field potential (LFP) and cells in the superficial layers of the MEC ( $n = 90$  cells) and in the hippocampus ( $n = 64$ ) during four consecutive 10-min recording sessions (Fig. 1A) (19, 20). After the first two 10-min sessions, we manipulated theta oscillations by microinfusions of lidocaine into the medial septum (fig. S1). Such infusions substantially reduced the amplitude and frequency of theta oscillations in the MEC and the hippocampus (Fig. 1 and fig. S2).

Would the spatial firing characteristics of cells predict their response to the manipulation? We first selected grid cells by measuring the hexagonal regularity of firing (i.e., “gridness”), only

accepting cells with scores higher than the 99th percentile of shuffled data. The periodic spatial firing pattern of grid cells (their gridness) vanished during the period of reduced theta (Fig. 2 and figs. S3 and S4). The firing rates of grid cells decreased during periods of theta reduction (Fig. 2C), whereas head-direction cells did not show changes in mean firing rate (Fig. 3, A and D) or mean vector length (fig. S5).

The parallel decrease in gridness and firing rates raised the question whether grid patterns in fact persisted but were obscured from detection because of the limited number of spikes. We therefore performed additional analysis. First, we observed that the firing rates of a subset of grid cells recovered in advance of their grid patterns and demonstrated that the two measurements were unrelated [correlation coefficient ( $r$ ) = 0.07, n.s.; fig. S6]. Second, the spikes that remained during periods of reduced theta occurred not only without spatial regularity but also at locations unrelated to the original grid pattern (Fig. 2, D and E). Finally, we randomly omitted spikes from

recording periods with higher firing rates to obtain spike trains with matching average rates for each 10-min recording. As intended, this resulted in a low firing rate for each recording segment ( $0.82 \pm 0.15$  to  $0.84 \pm 0.15$  Hz). We used these samples to recalculate gridness. As in the original sample, robust grid firing was seen in subsampled data before, but not after, theta oscillations were reduced (Fig. 2B and fig. S7).

Are theta oscillations thus required for sustaining any well-defined spatial firing? We selected MEC cells with spatial firing fields but without grid-like regularity [i.e., spatial nongrid cells (21–24)]. Their spatial firing locations were partially preserved, while their firing rates decreased to a similar extent as those of grid cells (Fig. 3, A to C, and fig. S8). In addition, many cells in the MEC continued to fire rhythmically as shown in autocorrelograms but at oscillation frequencies that decreased by 0.67 Hz ( $t = 3.31$ ,  $P < 0.01$ ). A similar decrease was seen for interneurons in the MEC and for hippocampal cells (fig. S2), indicating a downshift in the intrinsic oscillation frequen-

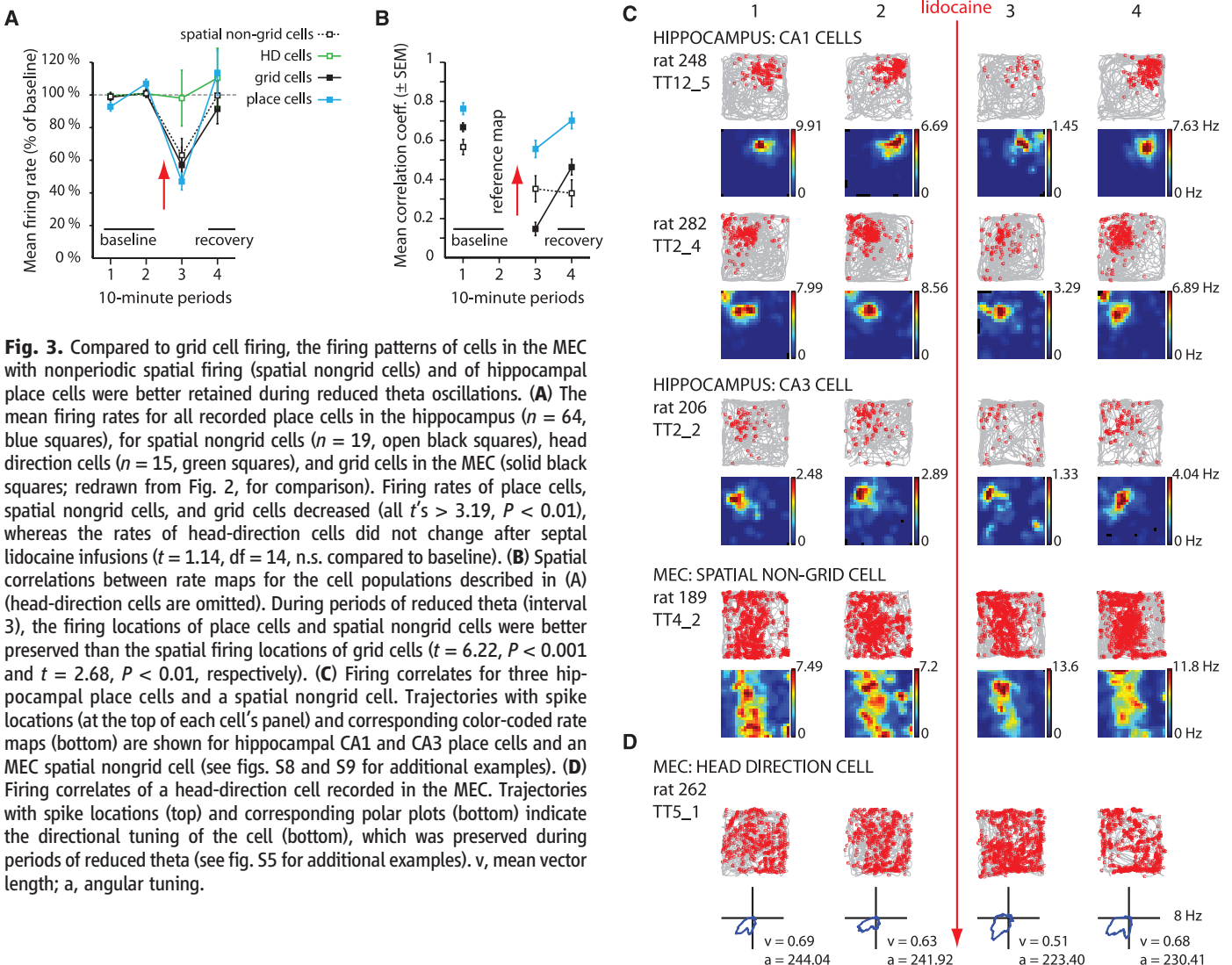


**Fig. 3.** Compared to grid cell firing, the firing patterns of cells in the MEC with nonperiodic spatial firing (spatial nongrid cells) and of hippocampal place cells were better retained during reduced theta oscillations. **(A)** The mean firing rates for all recorded place cells in the hippocampus ( $n = 64$ , blue squares), for spatial nongrid cells ( $n = 19$ , open black squares), head direction cells ( $n = 15$ , green squares), and grid cells in the MEC (solid black squares; redrawn from Fig. 2, for comparison). Firing rates of place cells, spatial nongrid cells, and grid cells decreased (all  $t$ 's  $> 3.19$ ,  $P < 0.01$ ), whereas the rates of head-direction cells did not change after septal lidocaine infusions ( $t = 1.14$ ,  $df = 14$ , n.s. compared to baseline). **(B)** Spatial correlations between rate maps for the cell populations described in (A) (head-direction cells are omitted). During periods of reduced theta (interval 3), the firing locations of place cells and spatial nongrid cells were better preserved than the spatial firing locations of grid cells ( $t = 6.22$ ,  $P < 0.001$  and  $t = 2.68$ ,  $P < 0.01$ , respectively). **(C)** Firing correlates for three hippocampal place cells and a spatial nongrid cell. Trajectories with spike locations (at the top of each cell's panel) and corresponding color-coded rate maps (bottom) are shown for hippocampal CA1 and CA3 place cells and an MEC spatial nongrid cell (see figs. S8 and S9 for additional examples). **(D)** Firing correlates of a head-direction cell recorded in the MEC. Trajectories with spike locations (top) and corresponding polar plots (bottom) indicate the directional tuning of the cell (bottom), which was preserved during periods of reduced theta (see fig. S5 for additional examples).  $v$ , mean vector length;  $a$ , angular tuning.

cy of the hippocampo-entorhinal circuitry (25) when pacing by septal inputs was reduced.

Hippocampal place cells are also spatially modulated cells without periodicity in their firing pattern. Their spatial firing patterns are partially affected in the radial maze after septal inactivation and in the open field during reduced cholinergic neurotransmission (26, 27). For comparisons with MEC cells, we therefore recorded from hippocampal place cells in the same experimental design while reducing theta oscillations to the same extent as in MEC recordings (fig. S2) (20). We observed a substantial decrease in the firing rate of hippocampal place cells, and the spike trains of individual hippocampal cells showed reduced theta modulation (Fig. 3A and fig. S2). Place fields remained well-defined and at corresponding locations (Fig. 3, B and C, figs. S9 and S10, and table S1).

By silencing the septal area, we diminished theta oscillations in the entorhino-hippocampal circuitry and showed that the periodic firing of grid cells does not persist. Subcortical inputs to hippocampus and parahippocampal cortices are thus essential not only for theta oscillations but also for sustaining the spatial periodicity of grid cells. These findings are consistent with the theory that grid cells emerge from the interference between multiple precisely tuned theta oscillations within individual cells (12–14). Alternatively, the silencing of septal inputs to the MEC might result in the desynchronization of grid cells, so that the local network of cortical cells can no longer generate oscillatory interference (12, 28). Our data also identified a subpopulation of grid cells that do not regain their spatial regularity when theta oscillations recover (fig. S6). This suggests that a fraction of grid cells might not be directly participating in the generation of grid patterns, but rather becomes associated with other grid cells by plasticity-dependent mechanisms.

A parallel study (29) has independently discovered that grid cell firing does not persist during reduced theta oscillations and that other cell types are less affected. Together, our results show that the neuronal network mechanisms that sustain the periodic spatial firing of grid cells are different from those required for other firing correlates in the entorhino-hippocampal circuitry, including head-direction cells and place cells. The effect on grid cells is likely not mediated through effects of septal silencing on the firing of hippocampal place cells, because it has been shown that grid cell firing initially remains intact after the hippocampus has been silenced (30). Subcortical inputs are therefore necessary for the neural computations in the MEC that generate grid-like, periodic, spatial firing patterns, whereas the firing locations of place cells largely persist after inputs from grid cells and from subcortical areas to the hippocampus have substantially changed.

#### References and Notes

1. C. M. Gray, P. König, A. K. Engel, W. Singer, *Nature* **338**, 334 (1989).
2. L. L. Colgin *et al.*, *Nature* **462**, 353 (2009).

3. A. D. Ekstrom *et al.*, *Hippocampus* **15**, 881 (2005).
4. W. Klimesch, *Brain Res. Brain Res. Rev.* **29**, 169 (1999).
5. R. I. Wilson, G. Laurent, *J. Neurosci.* **25**, 9069 (2005).
6. J. O'Keefe, L. Nadel, *The Hippocampus as a Cognitive Map* (Oxford Univ. Press, Oxford, 1978).
7. J. O'Keefe, J. Dostrovsky, *Brain Res.* **34**, 171 (1971).
8. T. Hafting, M. Fyhn, S. Molden, M. B. Moser, E. I. Moser, *Nature* **436**, 801 (2005).
9. J. S. Taube, R. U. Muller, J. B. Ranck Jr., *J. Neurosci.* **10**, 420 (1990).
10. C. N. Boccara *et al.*, *Nat. Neurosci.* **13**, 987 (2010).
11. C. H. Vanderwolf, *Electroencephalogr. Clin. Neurophysiol.* **26**, 407 (1969).
12. N. Burgess, C. Barry, J. O'Keefe, *Hippocampus* **17**, 801 (2007).
13. M. E. Hasselmo, L. M. Giocomo, E. A. Zilli, *Hippocampus* **17**, 1252 (2007).
14. J. O'Keefe, N. Burgess, *Hippocampus* **15**, 853 (2005).
15. H. Petsche, C. Stumpf, G. Gogolak, *Electroencephalogr. Clin. Neurophysiol.* **14**, 202 (1962).
16. S. J. Mizumori, C. A. Barnes, B. L. McNaughton, *Brain Res.* **500**, 99 (1989).
17. R. M. Yoder, K. C. Pang, *Hippocampus* **15**, 381 (2005).
18. K. J. Jeffery, J. G. Donnett, J. O'Keefe, *Neuroreport* **6**, 2166 (1995).
19. Materials and methods are available as supporting material on Science Online.
20. Hippocampal and MEC cells were recorded in separate experiments (except for the data in fig. S10). In the MEC, grid cells ( $n = 26$ ) and other cell types ( $n = 27$ ) simultaneously with grid cells, and  $n = 37$  without grid cells) were recorded.
21. The firing fields of a subset of MEC cells had the stripe-like appearance of boundary vector cells, but only 6 of 19 fired maximally at the border. A field size

22. N. Burgess, J. O'Keefe, *Hippocampus* **6**, 749 (1996).
23. C. Lever, S. Burton, A. Jeewajee, J. O'Keefe, N. Burgess, *J. Neurosci.* **29**, 9771 (2009).
24. T. Solstad, C. N. Boccara, E. Kropff, M. B. Moser, E. I. Moser, *Science* **322**, 1865 (2008).
25. C. T. Dickson, J. Magistretti, M. Shalinsky, B. Hamam, A. Alonso, *Ann. N. Y. Acad. Sci.* **911**, 127 (2000).
26. S. J. Mizumori, B. L. McNaughton, C. A. Barnes, K. B. Fox, *J. Neurosci.* **9**, 3915 (1989).
27. E. Brazhnik, R. Borgnis, R. U. Muller, S. E. Fox, *J. Neurosci.* **24**, 9313 (2004).
28. E. A. Zilli, M. E. Hasselmo, *J. Neurosci.* **30**, 13850 (2010).
29. M. P. Brandon *et al.*, *Science* **332**, 595 (2011).
30. T. Hafting, M. Fyhn, T. Bonnevie, M. B. Moser, E. I. Moser, *Nature* **453**, 1248 (2008).
31. The authors thank T. Solstad and E. Mankin for Matlab scripts and M. Hasselmo, L. Squire, and M. Scanziani for comments and discussions. Supported by the Walter F. Heiligenberg Professorship, NSF/NIH/Bundesministerium für Bildung und Forschung grant 1010463, Ellison Medical Foundation grant AG-NS-0724-10, the Alfred P. Sloan Foundation, and Alzheimer's Association grant NIRG-09-133414.

#### Supporting Online Material

www.sciencemag.org/cgi/content/full/332/6029/592/DC1  
Materials and Methods  
Figs. S1 to S11  
Table S1  
References

14 December 2010; accepted 24 March 2011  
10.1126/science.1201685

## Reduction of Theta Rhythm Dissociates Grid Cell Spatial Periodicity from Directional Tuning

Mark P. Brandon,\* Andrew R. Bogaard, Christopher P. Libby, Michael A. Connerney, Kishan Gupta, Michael E. Hasselmo\*

Grid cells recorded in the medial entorhinal cortex of freely moving rats exhibit firing at regular spatial locations and temporal modulation with theta rhythm oscillations (4 to 11 hertz). We analyzed grid cell spatial coding during reduction of network theta rhythm oscillations caused by medial septum (MS) inactivation with muscimol. During MS inactivation, grid cells lost their spatial periodicity, whereas head-direction cells maintained their selectivity. Conjunctive grid-by-head-direction cells lost grid cell spatial periodicity but retained head-direction specificity. All cells showed reduced rhythmicity in autocorrelations and cross-correlations. This supports the hypothesis that spatial coding by grid cells requires theta oscillations, and dissociates the mechanisms underlying the generation of entorhinal grid cell periodicity and head-direction selectivity.

The role of oscillations in neural coding is controversial. Theta frequency oscillations (4 to 11 Hz) play an important role in memory behavior (1–4) and code spatial location by the precession of spike timing relative to theta

oscillations (theta phase precession) in the hippocampus (5, 6) and medial entorhinal cortex (MEC) (7). However, disagreement remains about whether theta oscillations are critical to spatial coding by neurons. Grid cells (8, 9) in the MEC provide a powerful example for testing the theoretical role of oscillations in neural coding. Some computational models of grid cells use network theta rhythm oscillations to generate grid cell spatial periodicity (10, 11). These models simulate the phase of spike timing in grid cells (7)

Center for Memory and Brain, Department of Psychology, Graduate Program for Neuroscience, Boston University, 2 Cummings Street, Boston, MA 02215, USA.

\*To whom correspondence should be addressed. E-mail: hasselmo@bu.edu (M.E.H.); markpb68@bu.edu (M.P.B.)